International Journal of Mass Spectrometry xxx (2017) xxx–xxx

Contents lists available at ScienceDirect

International Journal of Mass Spectrometry

journal homepage: www.elsevier.com/locate/ijms

Discovery and targeted monitoring of polychlorinated biphenyl metabolites in blood plasma using LC-TIMS-TOF MS

Kendra J. Adams [a], Natalie F. Smith [a], Cesar E. Ramirez [a], Francisco Fernandez-Lima [a,b,*]

[a] Department of Chemistry and Biochemistry, Florida International University, Miami, FL 33199, United States
[b] Biomolecular Sciences Institute, Florida International University, Miami, FL 33199, United States

ARTICLE INFO

Article history:
Received 31 May 2017
Received in revised form 18 October 2017
Accepted 16 November 2017
Available online xxx

Keywords:
Metabolites
Trapped ion mobility spectrometry
Mass spectrometry
Discovery and targeted monitoring

ABSTRACT

In the present work, the potential for rapid, targeted analysis of hydroxylated metabolites of polychlorinated biphenyls (OH-PCBs) in diluted human blood plasma using liquid chromatography coupled with trapped ion mobility spectrometry and TOF high resolution mass spectrometry (LC-TIMS-TOF MS) was evaluated. Experimental OH-PCB collisional cross section (CCS_{N2}) and gas-phase candidate structures (<3% error) are reported for the first time and used, in addition to the LC retention time and accurate *m/z*, as OH-PCB identification features in order to increase the detection selectivity. The proposed LC-TIMS-TOF MS workflow combines a "dilute-and-shoot" sample preparation strategy, a robust liquid chromatography step, a high-resolving power mobility separation (R ~ 150–250) and high-resolution mass spectrometry (R ~ 30–40k) for the separation, identification and quantification of common OH-PCB isomers with limits of detection comparable to traditional workflows (e.g., LOD and LOQ of ~10 pg/mL and ~50 pg/mL, respectively). The higher selectivity and low detection limits provides multiple advantages compared to current methodologies that typically require long, labor-intensive preparation and/or derivatization steps prior to gas or liquid chromatography–mass spectrometry.

1. Introduction

Polychlorinated biphenyls (PCBs) are endocrine disruptors that have antagonistic effects on reproductive, neurological, and immune systems in humans and wildlife [1]. Production of PCBs was banned in the United States during the 1970's; however, these compounds are still found in the environment and considered persistent organic pollutants [2–4]. PCBs are metabolized to hydroxylated PCBs (OH-PCBs) and/or methyl sulfone PCBs (MeSO-PCBs) via cytochrome P-450 [3]. Hydroxylation occurs through epoxidation, which forms an arene oxide intermediate followed by the formation of a hydroxyl-PCB [3,5–9]. The location of the hydroxyl group on the biphenyl rings is directly correlated to the analyte toxicity [1,10]. When the hydroxylation occurs at *para*- or *meta*- positions in combination with an adjacent chlorine atom, the compound bears significant resemblance to thyroid hormones, triiodothyronine (T3) and thyroxine (T4) [11,12]. The OH-PCBs competitively bind to the thyroid hormone receptors and can have up to 10-times higher binding affinity to transthyretin than the hormones themselves [5,11,12]. This competitive binding causes a high retention of OH-PCBs in blood plasma, resulting in various toxicological effects such as neurodevelopment, carcinogenicity, and reproductive impairment [5,9,13].

The most common experimental methods for the separation and detection of PCB metabolites are gas chromatography and liquid chromatography coupled to mass spectrometry (GC–MS and LC–MS). Traditionally, GC–MS analysis has been utilized for PCB metabolites, although, to analyze phenolic compounds, derivatization is required [7,14–16]. Other studies have proposed the use of LC–MS/MS strategies for separation, detection, and quantification of OH-PCBs in humans and wildlife [7,8,15,17,18]. Typically, before introducing the sample to a LC–MS system, an analyte extraction and sample cleanup protocol is required. Several methods of extraction have been utilized for various biological matrices such as whole blood, serum and plasma, most of which include liquid–liquid extraction followed by partitioning [18]. Cleanup procedures have also been implemented using silica columns [18]. After the lengthy extraction and cleanup steps for biological samples, a secondary cleanup is typically performed using solid phase extraction immediately prior to separation in the analytical column [8]. The addition of these extraction and cleanup procedures significantly increases

* Corresponding author at: Department of chemistry and Biochemistry, Florida International University, Miami, FL 33199, United States.
E-mail address: fernandf@fiu.edu (F. Fernandez-Lima).

https://doi.org/10.1016/j.ijms.2017.11.009
1387-3806/

the analysis time and typically require the use of added resources throughout the analytical procedure. Despite the progress made over the years, there is a clear need for simplified analytical workflows with enhanced selectivity and increased sensitivity.

An alternative approach includes the use of gas-phase, post-ionization separations such as ion mobility spectrometry coupled to mass spectrometry (IMS-MS), which promises further gains in speed, sensitivity and selectivity for the analysis of complex biological mixtures [19,20]. Specifically, the added mobility dimension of separation yields an increase in peak coverage [21–24], a factor that has often inhibited the analysis of complex mixtures with MS-only detection. The ion's mobility gives information on its size and shape via the momentum transfer ion-neutral collision cross section (CCS) [25]. While this description holds true for most contemporary IMS analyzers (e.g., periodic focusing DC ion guide [26–28], segmented quadrupole drift cell [29], multi-stage IMS [30–32], transient wave ion guide [33,34] and SLIM devices [35]), a common pursuit has been to increase IMS resolving power and ion transmission [36–44]. Since the introduction of TIMS-MS in 2011 [45,46], our group [47–60], and others [61–70] have shown the potential of TIMS-MS for gas-phase separation and for molecular structural elucidation. In particular, we have demonstrated the advantages of TIMS for screening [47] and targeted [48] analysis of molecular ions from complex chemical mixtures; the study of isomerization kinetics of small molecules [49,51,52], peptides [50], DNA [59], proteins [54,55], DNA-protein complexes and protein–protein complexes in their native and denatured states [58]. In a more recent report, we showed the isomer separation of polybrominated diphenyl ether metabolites using nanoESI-TIMS-TOF MS with mobility resolving powers of up to 400 (the highest reported mobility resolving power for singly charged species) [56].

In the present work, the potential for rapid, targeted analysis of hydroxylated metabolites of polychlorinated biphenyls (OH-PCB) using online liquid chromatography in tandem with trapped ion mobility spectrometry and TOF mass spectrometry (LC-TIMS-TOF MS) was studied for the first time. Several OH-PCB congeners, ranging from penta-chlorinated to hepta-chlorinated biphenyls, were studied as single standards, mixtures and in the presence of a complex matrix-human blood plasma. The advantages of LC-TIMS-TOF MS over traditional GC–MS and LC–MS/MS analysis are discussed based on analysis time, selectivity and sensitivity.

2. Experimental methods

2.1. Materials and reagents

All solvents were purchased from Fisher Scientific (Pittsburg, PA) and were of Optima LC–MS quality or better. Hydroxylated polychlorinated biphenyl standards were purchased from Wellington Laboratories (ON, Canada) and Accustandard, Inc. (New Haven, CT, USA). Pooled human plasma was purchased from Innovative Research (Novi, MI, USA). Nine OH-PCBs were used in this study: 2,3,3′,4′,5-Pentachloro-4-biphenylol (4-OH CB 107), 2′,3,3′,4′,5-Pentachloro-4-biphenylol (4-OH CB 108), and 2,3′,4,4′,5-Pentachloro-3-biphenylol (3-OH CB 118), 2,2′,3,3′,4′,5-Hexachloro-4-biphenylol (4-OH CB 130), 2,2′,3′,4,4′,5-Hexachloro-3-biphenylol (3-OH CB 138), and 2,2′,3,4′,5,5′-Hexachloro-4-biphenylol (4-OH CB 146), 2,2′,3,3′,4′,5,5′-Heptachloro-4-biphenylol (4-OH-PCB 172), 2,2′,3′,4,4′,5,5′-Heptachloro-3-biphenylol (3-OH CB 180), and 2,2′,3,4′,5,5′,6-Heptachloro-4-biphenylol (4-OH CB 187). Binary isomer mixtures were created by mixing equal volumes of the individual standards.

2.2. OH-PCB human blood plasma samples

Pooled human plasma was removed from storage at −20 °C and thawed on ice. A 150 μL aliquot of plasma was mixed with an equal amount of acetonitrile and spiked with a mixture of OH-PCBs for final concentrations of 0, 10, 25, 50, 100, 500, 1000, 5000, and 10,000 pg/mL. It has been reported that acetonitrile would break the cell membranes, as well as precipitate the large proteins as a way to increase extortion of the intracellular components [71,72]. Three OH-PCB standards were used for the spike mixture: 4-Hydroxy-2′,3,3′,4′,5′-pentachlorobiphenyl, 5-Hydroxy-2,2′,3,4,4′,5′-hexachlorobiphenyl and 4′-Hydroxy-2,2′,3,3′,4,5,5′-heptachlorobiphenyl. Samples were vortex, mixed for 1 min and centrifuged at 4 °C for 10 min at 4500 rpm to remove the proteins from the aqueous layer. Following centrifugation, the supernatant was transferred without any further clean-up, to LC vials with borosilicate glass inserts for analysis.

2.3. LC-ESI-TIMS-MS analysis

The LC-ESI-TIMS-TOF MS analysis was performed using a custom-built TIMS-TOF MS based on the maXis impact Q-ToF MS (Bruker Daltonics Inc, Billerica, MA). Sample injection (40 μL) and LC separation was performed on a Shimadzu Prominence HPLC system consisting of two 20AD pumps, a SIL-20AC auto-sampler and a CTO 20-A column oven held at 40° C (Kyoto, Japan). An Onyx Monolithic C18 HPLC column (100 × 4.6 mm) was used protected by an Onyx guard column (5 × 4.6 mm), both from Phenomenex (Torrance, CA, USA). A 15-min gradient separation was performed at a variable flow rate (2 mL/min for two minutes and then decreased to 1 mL/min for the remaining 13 min of the program) using water and acetonitrile. Mobile phase composition was changed as follows: hold 10% B for two minutes; increase to 97% B in three minutes and hold for 6.75 min; return to 10% B in 0.5 min and hold for 2.75 min for re-equilibration. Samples were ionized and introduced into the TIMS-TOF-MS using an ionBooster ESI source in negative ion mode (Bruker Daltonics Inc, Billerica, MA). Typical ionBooster operating conditions were 1000 V capillary voltage, 400 V end plate offset, 300 V charging voltage, 4.1 bar nebulizer pressure, 3.0 L/min dry gas, 270 °C dry heater, and 400 °C vaporizer.

A detailed overview of the TIMS analyzer and its operation can be found elsewhere [45,46,53]. The nitrogen bath gas flow is defined by the pressure difference between entrance funnel P_1 = 2.7 mbar and the exit funnel P_2 = 1.1 mbar at *ca.* 300 K. The TIMS analyzer is comprised of three regions: an entrance funnel, analyzer tunnel (46 mm axial length), and exit funnel. A 2040 kHz and 250 Vpp RF potential was applied to each section creating a dipolar field in the funnel regions and a quadrupolar field inside the tunnel. During TIMS operation, multiple ion species are trapped simultaneously at different E values resulting from a voltage gradient applied across the TIMS tunnel. After thermalization, species are eluted from the TIMS cell by decreasing the electric field in stepwise decrements (referred to as the "ramp"). The TIMS cell was operated using a fill/ramp sequence of 10/100 ms or 100/100 ms for a 10% and 50% duty cycle for better chromatography and higher sensitivity, respectively. The TOF analyzer was operated at 10 kHz (m/z 100–1500). The data was segmented in LC frames over 10 analysis cycles yielding an LC-TIMS-TOF MS step size of ~2 s. Mobility calibration was performed using the Tuning Mix calibration standard (G24221A, Agilent Technologies, Santa Clara, CA) in positive ion mode (e.g., m/z 322, $K_0 = 1.376\ cm^2\ V^{-1}\ s^{-1}$ and m/z 622, $K_0 = 1.013\ cm^2\ V^{-1}\ s^{-1}$) resulting in A = 231.064 for the instrumental and method conditions employed [53]. The TIMS operation was controlled using in-house software, written in National Instruments Lab VIEW, and synchronized with the maXis Impact Q-ToF acquisition program [45].

Please cite this article in press as: K.J. Adams, et al., Discovery and targeted monitoring of polychlorinated biphenyl metabolites in blood plasma using LC-TIMS-TOF MS, Int. J. Mass Spectrom. (2017), https://doi.org/10.1016/j.ijms.2017.11.009

Reduced mobility values (K_0) were correlated with collisional cross section (Ω) using the equation:

$$\Omega = \frac{(18\pi)^{1/2}}{16}\frac{z}{(k_B T)^{1/2}}\left[\frac{1}{m_I}+\frac{1}{m_b}\right]^{1/2}\frac{1}{K_0}\frac{1}{N^*} \quad (1)$$

where z is the charge of the ion, k_B is the Boltzmann constant, N^* is the number density of the bath gas, and m_I and m_b refer to the masses of the ion and bath gas, respectively [25]. All resolving power ($R = \Omega/\Delta\Omega$) values were determined from Gaussian peak fits after smoothing of peaks (Savitzky-Golay with 30-80 points of window) using OriginPro (version 8.0). LC-TIMS-TOF MS data were processed using Data Analysis software v. 5.0 (Bruker Daltonics Inc, Billerica, MA) and the calibration plots utilized mobility selected data in the *m/z* domain.

2.4. Theoretical calculations

A pool of candidate structures were proposed for each OH-PCB analyzed using TIMS-TOF MS. Final structures were optimized at the DFT/B3LYP/6-311G(d,p) level using Gaussian software [73]. Vibrational frequencies were calculated to guarantee that the optimized structures correspond to actual minima in the energy space, and zero-point energy corrections were applied to calculate the relative stability between the structures. Theoretical ion-neutral collision cross sections were calculated using iMOS [74,75] software for nitrogen as a bath gas at ca. 300 K. Partial atomic charges were calculated using the Merz-Singh-Kollman scheme constrained to the molecular dipole moment [76,77].

3. Results and discussion

The TIMS-TOF MS analysis of the penta-chlorinated (4-OH CB 107, 4-OH CB 108, and 3-OH CB 118), hexa-chlorinated (4-OH CB 130, 3-OH CB 138, and 4-OH CB 146), and hepta-chlorinated (4-OH CB 172, 3-OH CB 180, and 4-OH CB 187) biphenyls is summarized in Fig. 1 and Table 1. Inspection of the TIMS-TOF MS spectra showed the presence of deprotonated molecular ions $[M-H]^-$ with isotope patterns characteristics of compounds with five, six and seven chlorine atoms. Inspection of the corresponding mobility profiles for the single standards showed the presence of a single mobility band, with resolving powers of $R \sim 150$. Experimental CCS are reported for all the analyzed single standards (Table 1). Inspection of Table 1 shows that there are very small CCS differences between the penta- (<0.4%), hexa- (<0.1%) and hepta- (<1.1%) chlorinated biphenyls. For example, the penta-CBs have an experimental CCS of 165.0 Å^2, 165.2 Å^2 and 165.6 Å^2 for the 4-OH CB 107, 4-OH CB 108 and 4-OH CB 118, respectively. Calculated CCS for the penta-CB proposed candidate structures show good agreement with the experimental CCS values (<3% difference). The hexa-CBs have an experimental CCS of 170.0 Å^2, 170.1 Å^2 and 170.2 Å^2 for the 4-OH CB 130, 3-OH CB 138 and 4-OH CB 146, respectively. Calculated CCS for the hexa-CB proposed candidate structures show good agreement with the experimental CCS values (<3% difference). The hepta-CBs have an experimental CCS of 172.6 Å^2, 173.4 Å^2 and 171.4 Å^2 for the 4- OH CB 172, 3-OH CB 180 and 4-OH CB 187, respectively. Calculated CCS values for the hepta-CB proposed candidate structures show good agreement with the experimental CCS (<2% difference).

When analyzed as binary mixtures, mobility separation was not observed between the penta-CBs (4-OH CB 107, 4-OH CB 108 and 3-OH CB 118) and hexa-CBs (4-OH CB 130, 3-OH CB 138, and 4-OH CB146). We attribute these results to the similarity in CCS between the isomers (Table 1). The separation of these compounds is analytically challenging, and only attempts using SPE-LC–MS/MS has been shown to separate the penta-CBs 3-OH CB 118 to the 4-OH CB107/108 [8,17] and the hexa-CBs 4-OH CB 130 to the 4-OH CB146/138 [8,17,78]. Moreover, baseline mobility separation

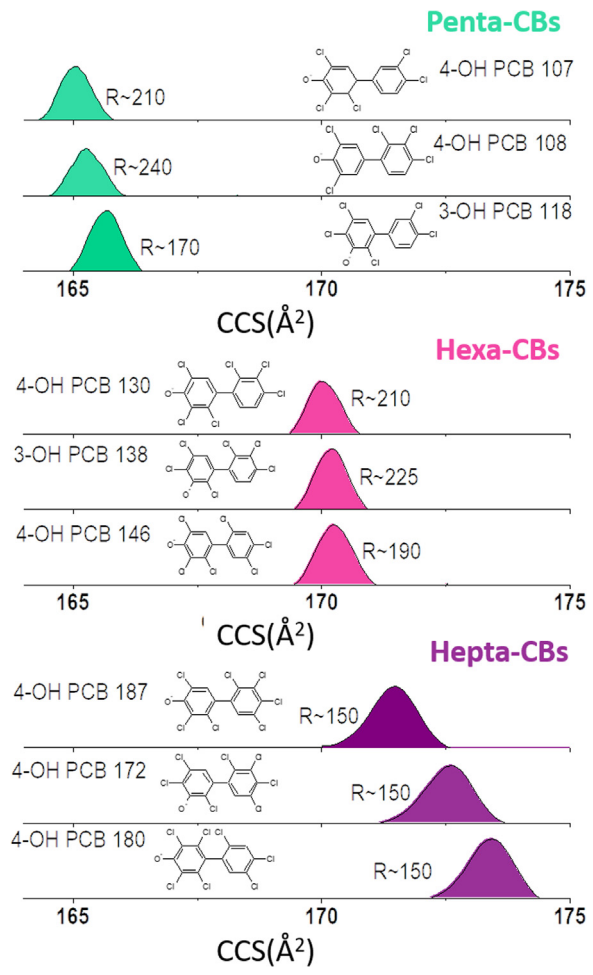

Fig. 1. Typical mobility profiles of single standards of penta-, hexa- and hepta-CBs.

was achieved for the case of the binary mixtures of the hepta-CBs with a mobility resolving power of $R \sim 150$ for the case of 4-OH CB 187 and 4-OH-CB172/180; however, mobility separation was not observed for the case of 4-OH CB 172/180 (Fig. 2). This mobility separation trend shows similarities with results observed using SPE-LC–MS/MS, where baseline separation is only observed between 4-OH CB 187 and 4-OH CB 172/180 [8].

To reduce sample preparation steps and maximize throughput a "dilute-and-shoot" strategy was adopted. Previous studies for extraction of OH-PCBs from plasma involve the use of preliminary extraction and cleanup steps followed by lengthy chromatographic analyses [7,8,15,17,79]. The proposed method uses a quick clean-up step using acetonitrile to precipitate the proteins, followed by centrifugation. The supernatant was injected into the LC system without further preparation steps for three-dimensional separation in chromatographic, ion mobility and mass spectrometric domains. The short LC method was developed using an Onyx Monolithic C18 column, which has been used previously for direct plasma injections and thus was selected to account for minimal sample preparation and clean-up prior to LC-TIMS-TOF MS analysis. The column output was combined with the ionBooster source to allow high eluent flow-rates (~1 mL/min). In Fig. 3, a two-dimensional IMS-MS plot is shown for samples containing 2 ppb of a 9-component mixture of OH-PCBs in water (3a) and plasma (3b). The marked regions pertain to the penta-, hexa- and hepta-CBs (Fig. 3). Inspection of the 2D-IMS-MS of the water sample shows clear mobility and mass separation of the penta-, hexa-, and hepta-CBs (Fig. 3a). Inspection of the LC-TIMS-TOF MS data showed a two

Please cite this article in press as: K.J. Adams, et al., Discovery and targeted monitoring of polychlorinated biphenyl metabolites in blood plasma using LC-TIMS-TOF MS, Int. J. Mass Spectrom. (2017), https://doi.org/10.1016/j.ijms.2017.11.009

Table 1
List of experimental and theoretical *m/z* and CCS values for the penta-, hexa-, and hepta-CB considered in this study.

Name	Chemical Formula	Theoretical *m/z* $[M-H]^-$	Experimental *m/z* $[M-H]^-$	Error (ppm)	Theoretical CCS ($Å^2$)	Experimental CCS (A^2)
4 OH 107	$C_{12}H_5Cl_5O$	340.8681	340.8682	0.293	161.3	165.0
4 OH 108	$C_{12}H_5Cl_5O$				161.2	165.2
3 OH 118	$C_{12}H_5Cl_5O$				161.1	165.6
4 OH 130	$C_{12}H_4Cl_6O$	374.8291	374.8291	0.000	164.1	170.0
3 OH 138	$C_{12}H_4Cl_6O$				165.0	170.1
4 OH 146	$C_{12}H_4Cl_6O$				166.0	170.2
4 OH 172	$C_{12}H_3Cl_7O$	408.7901	408.7905	0.975	171.0	172.6
3 OH 180	$C_{12}H_3Cl_7O$				171.0	173.4
4 OH 187	$C_{12}H_3Cl_7O$				171.3	171.4

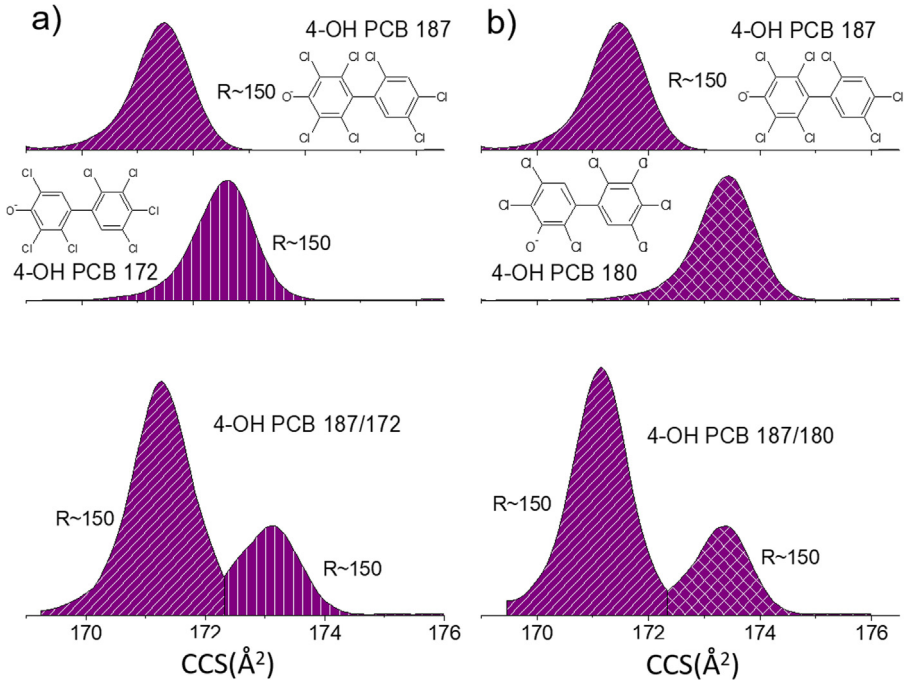

Fig. 2. Typical mobility profiles of the single standards and binary mixtures for the hepta-CBs.

band chromatographic separation for the hexa- and hepta-CBs, and a single chromatographic band (RT = 7.18 min) for the penta-CBs. For example, the extracted ion chromatogram (EIC) for the hexa-CBs (*m/z* 374.8291) and the hepta-CBs (*m/z* 408.7905) showed the separation of 4-OH CB 130 (RT = 7.22 min) to the 4-OH CB 146/138 (RT = 7.31 min) and 4-OH CB 187 (RT = 7.26 min) to the 4-OH CB 172/180, respectively (RT = 7.58 min). In the case of the plasma sample (Fig. 3b), multiple peaks are observed in the 2D-IMS MS domain; moreover, a clear separation of the targeted CBs from the plasma signal is observed in the IMS-MS domain. That is, high selectivity can be achieved during CBs detection on the proposed LC-TIMS-TOF MS workflow. For example, the advantages for higher selectivity of the LC-TIMS-TOF MS workflow are shown for the case of the hepta-CBs (Fig. 4) combining LC separation with accurate CCS and *m/z* measurements. It should be noted, that the CBs CCS values can be used as universal parameters for routine identifications, especially, in the cases where single standards of CBs are not accessible.

A comparative study of limit of detection (LOD) was conducted using traditional LC-ESI-TOF MS and the proposed LC-ESI-TIMS-TOF MS for quantitative detection of OH-PCBs. The main purpose of the study was to asses the effect of the TIMS separation, while all other experimental parameters are kept constant (Fig. 5). A nine-point matrix-matched calibration curve was built with peak intensity as a function of analyte concentration. A linear response for the penta-, hexa- and hepta- CBs from 0 to 5000 pg/mL was observed in both the LC-TOF MS and LC-TIMS-TOFMS analysis ($R^2 > 0.99$). Differences in the response curve are related to the duty cycle during the LC-TIMS-TOF MS measurements. That is, the use of single stage TIMS analyzer requires initial trapping followed by an elution step; during the elution step, new ions are not introduced in the analyzer which reduces the overall duty cycle. More recent versions of the TIMS-TOF MS operate using a dual TIMS analyzer which allows for almost 100% duty cycle [19]. The limit of detection (LOD, defined as the concentration that produces a signal three times higher than the background noise) for LC-TIMS-TOF MS was established at ~10 pg/mL for penta-CBs, hexa-CBs and hepta-CBs (Fig. 5). In contrast, the LOD for LC-TOF MS was obtained from the calibration plot at ~25 pg/mL, 2.5-times higher than the proposed technique (SI 2). This highlights the ability of the LC-TIMS-TOF MS to reduce the background interferences, cleaning up the detection of the targeted analytes during full scan detection (see Fig. 3). The limit of quantification (LOQ, defined as the concentration 10-times higher than the background noise of the un-spiked plasma) was established at 35 pg/mL for each analyte in spiked in plasma (Fig. 5), which is comparable to previous studies that employed GC and LC–MS/MS and reported LOQs between 1 and 100 pg/mL [8,18,78]. In particular, Quinete et al. [8] reported LOQs in the range of 20–50 pg/mL for the same analytes using a triple-quadrupole instrument to perform LC–MS/MS operating under multiple-reaction-monitoring (MRM) mode. The latter technique is considered the current standard for analytical quantitation, but has the inherent disadvantage of focusing only on pre-programmed

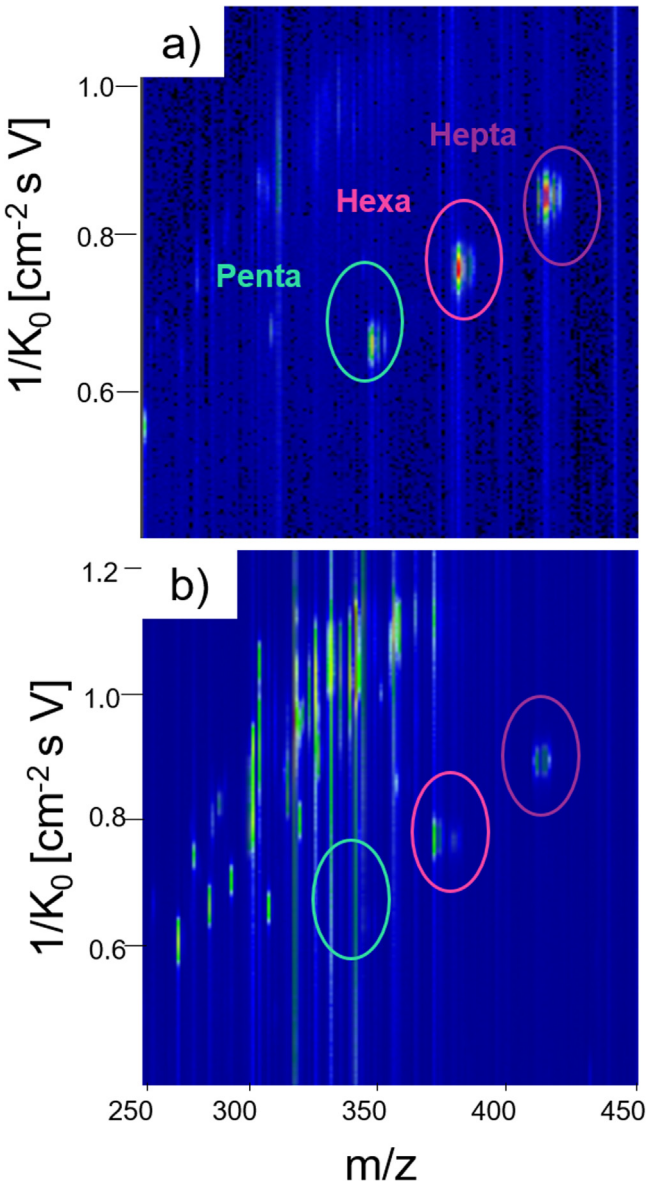

Fig. 3. Typical 2D-IMS-MS contour maps of the penta-, hexa-, and hepta-CBs in water (a) and in human blood plasma (b). Note the separation of the PCB signals from potential interferences in the IMS-MS domain.

transitions that leave out any untargeted species. Therefore, our presented LC-TIMS-TOF MS technique offers similar sensitivity to triple-quadrupole instruments with the added benefit of detection of untargeted species, enhancing the value of the obtained data by enabling back-interrogation of analytes of interest that may arise in the future. This high sensitivity using a full-scan detection can be attributed to the very high selectivity of the LC-TIMS-MS approach, which provides with very low background levels thanks to the separation of the analytes from isobaric interferences contained in plasma (see Fig. 3).

4. Conclusions

This work demonstrates a rapid screening of OH-PCBs in diluted human plasma using LC coupled with tandem trapped ion mobility spectrometry and TOF mass spectrometry (LC-TIMS-TOF MS) detection. Experimental collisional cross section and gas-phase candidate structures are reported for the first time for nine OH-PCB standards. The high mobility resolving power (R ~ 150–240) of the TIMS analyzer permitsbaseline separation of the hepta-CB 4-OH CB 187 and 4-OH-CB172/180, with differences in CCS of less 1%. Despite the high chemical complexity of human blood plasma samples (multiple peaks observed in the 2D-IMS MS domain during the analysis), a clear separation of the targeted CBs from other potential interferences is observed in the IMS-MS domain and used as quantitative signal with very high signal-to-noise ratios (LOD and LOQ of ~10 pg/mL and ~35 pg/mL, respectively). The LC-TIMS-TOF MS performance is comparable to established techniques such as LC–MS/MS which, unlike this work, do not allow for untargeted analysis and back-interrogation of data. High throughput is achieved by limiting sample clean-up steps to protein precipitation followed by direct supernatant injection on a monolithic column for HPLC separation and tandem ion mobility/mass spectrometric detection. The superior performance of this simplified LC-TIMS-TOF MS analytical workflow removes the need for labor-intensive

Please cite this article in press as: K.J. Adams, et al., Discovery and targeted monitoring of polychlorinated biphenyl metabolites in blood plasma using LC-TIMS-TOF MS, Int. J. Mass Spectrom. (2017), https://doi.org/10.1016/j.ijms.2017.11.009

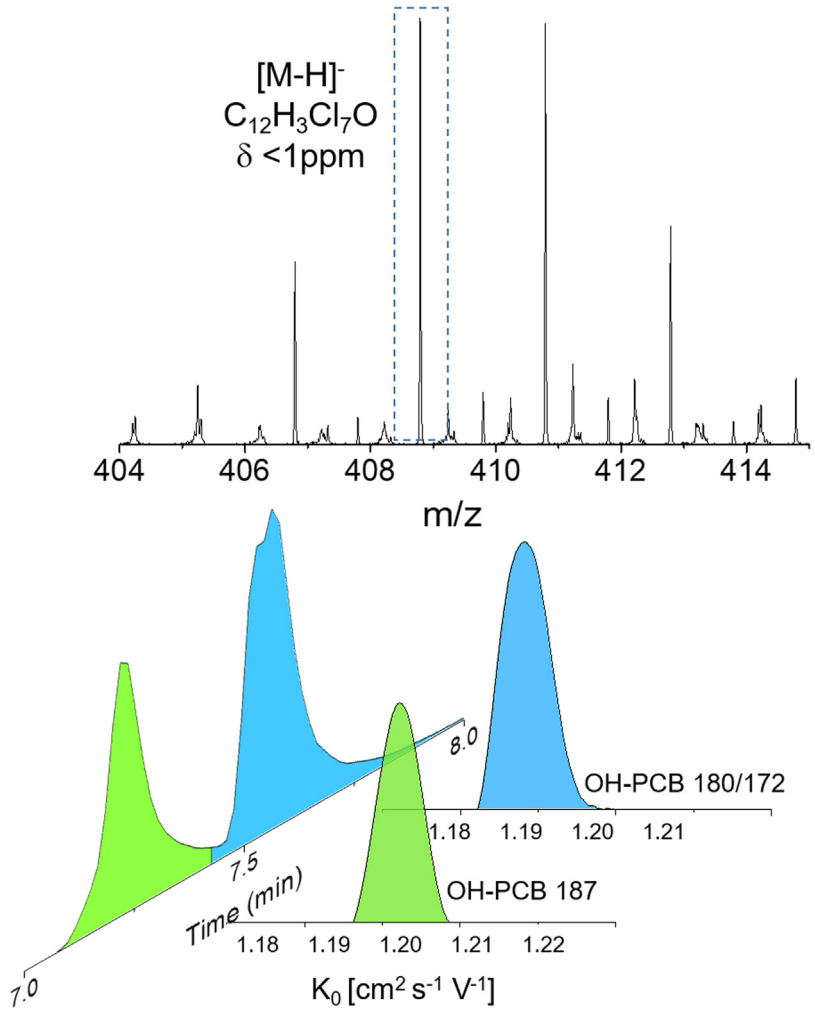

Fig. 4. Typical MS projection, LC projection and extracted ion mobility profiles for a mixture of hepta-CBs, (OH-PCB 187, OH-PCB 180 and OH-PCB 172), from the LC-TOF-MS analysis of the CBs in human blood plasma.

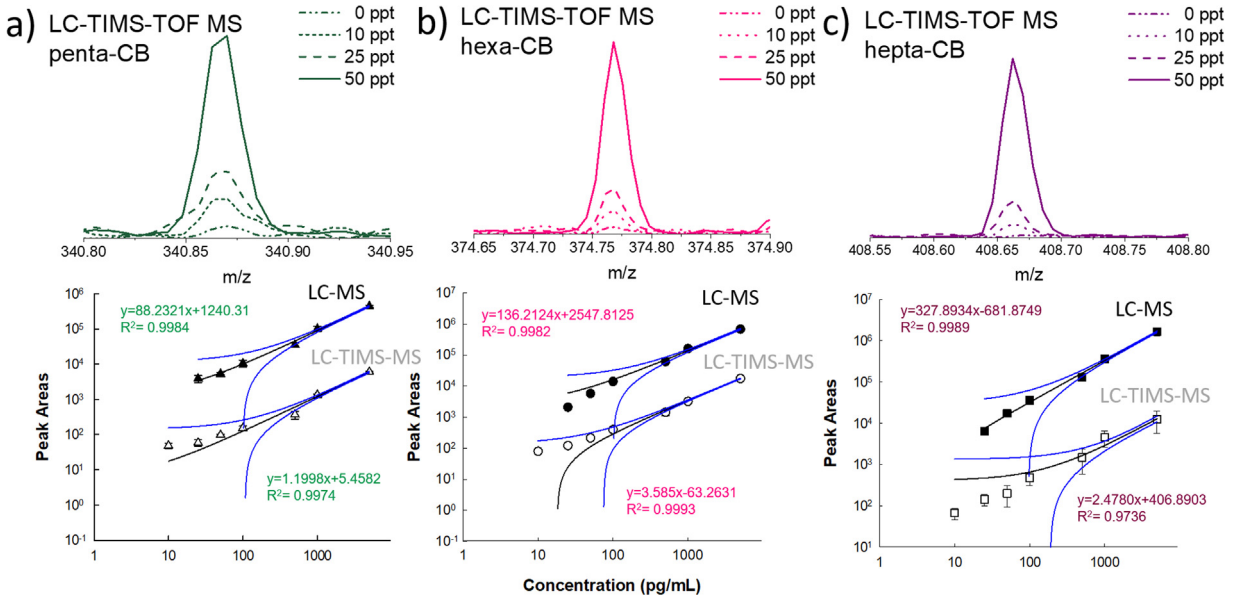

Fig. 5. Typical response curves for LC-TIMS-TOF MS as a function of a) penta- b) hexa- and c) hepta-CBs concentration in human blood plasma. Note the linear response for the penta-, hexa- and hepta- CBs from 0 to 5000 pg/mL in both the LC-TOF MS and LC-TIMS-TOFMS analysis.

Please cite this article in press as: K.J. Adams, et al., Discovery and targeted monitoring of polychlorinated biphenyl metabolites in blood plasma using LC-TIMS-TOF MS, Int. J. Mass Spectrom. (2017), https://doi.org/10.1016/j.ijms.2017.11.009

preparation steps to minimize chemical noise and represents a viable alternative to currently available methodologies.

Acknowledgements

This work was supported by the National Institutes of Health (R00GM106414), a Bruker Daltonics Inc. fellowship, and a National Science Foundation Division of Chemistry, under CAREER award CHE-1654274, with co-funding from the Division of Molecular and Cellular Biosciences to F.F.-L. The authors will also like to acknowledge the helpful discussions and technical support from Dr. Mark E. Ridgeway and Dr. Melvin A. Park from Bruker Daltonics Inc. during the development and installation of the custom-built TIMS-TOF MS instrument.

K.J.A. acknowledges the support from the FIU Dissertation Year Fellowship.

References

[1] N. Quinete, T. Schettgen, J. Bertram, T. Kraus, Occurrence and distribution of PCB metabolites in blood and their potential health effects in humans: a review, Environ. Sci. Pollut. Res. 21 (2014) 11951–11972.
[2] G. Ross, The public health implications of polychlorinated biphenyls (PCBs) in the environment, Ecotoxicol. Environ. Saf. 59 (2004) 275–291.
[3] I. Kania-Korwel, H.-J. Lehmler, Chiral polychlorinated biphenyls: absorption, metabolism and excretion–a review, Environ. Sci. Pollut. Res. 23 (2016) 2042–2057.
[4] M.L. Diamond, L. Melymuk, S.A. Csiszar, M. Robson, Estimation of PCB stocks, emissions, and urban fate: will our policies reduce concentrations and exposure? Environ. Sci. Technol. 44 (2010) 2777–2783.
[5] A. Bergman, E. Klasson-Wehler, H. Kuroki, Selective retention of hydroxylated PCB metabolites in blood, Environ. Health Perspect. 102 (1994) 464.
[6] H. Matthews, M. Anderson, Effect of chlorination on the distribution and excretion of polychlorinated biphenyls, Drug Metab. Dispos. 3 (1975) 371–380.
[7] R.J. Letcher, H.X. Li, S.G. Chu, Determination of hydroxylated polychlorinated biphenyls (HO-PCBs) in blood plasma by high-performance liquid chromatography-electrospray ionization-tandem quadrupole mass spectrometry, J. Anal. Toxicol. 29 (2005) 209–216.
[8] N. Quinete, T. Kraus, V.N. Belov, C. Aretz, A. Esser, T. Schettgen, Fast determination of hydroxylated polychlorinated biphenyls in human plasma by online solid phase extraction coupled to liquid chromatography–tandem mass spectrometry, Anal. Chim. Acta 888 (2015) 94–102.
[9] R.J. Letcher, E. Klasson-Wehler, A. Bergman, Methyl Sulfone and Hydroxylated Metabolites of Polychlorinated Biphenyls, In: vol. 3 Anthropogenic Compounds Part K, Springer, 2000, pp. 315–359.
[10] L.N. Kinch, N.V. Grishin, Evolution of protein structures and functions, Curr. Opin. Struct. Biol. 12 (2002) 400–408.
[11] A. Brouwer, D.C. Morse, M.C. Lans, A. Gerlienke Schuur, A.J. Murk, E. Klasson-Wehler, Å. Bergman, T.J. Visser, Interactions of persistent environmental organohalogens with the thyroid hormone system: mechanisms and possible consequences for animal and human health, Toxicol. Ind. Health 14 (1998) 59–84.
[12] M.C. Lans, E. Klasson-Wehler, M. Willemsen, E. Meussen, S. Safe, A. Brouwer, Structure-dependent competitive interaction of hydroxy-polychlorobiphenyls, -dibenzo-p-dioxins and -dibenzofurans with human transthyretin, Chem. Biol. Interact. 88 (1993) 7–21.
[13] H.E. Purkey, S.K. Palaninathan, K.C. Kent, C. Smith, S.H. Safe, J.C. Sacchettini, J.W. Kelly, Hydroxylated polychlorinated biphenyls selectively bind transthyretin in blood and inhibit amyloidogenesis: rationalizing rodent PCB toxicity, Chem. Biol. 11 (2004) 1719–1728.
[14] U. Berger, D. Herzke, T.M. Sandanger, Two trace analytical methods for determination of hydroxylated PCBs and other halogenated phenolic compounds in eggs from Norwegian birds of prey, Anal. Chem. 76 (2004) 441–452.
[15] R. Liang, Y. Zhao, Y. Su, W. Qin, Determination of hydroxylated polychlorinated biphenyls by offline solid-phase extraction-liquid chromatography–tandem mass spectrometry using a molecularly imprinted polymer as a sorbent for sample preconcentration, Talanta 144 (2015) 115–121.
[16] L. Hovander, T. Malmberg, M. Athanasiadou, I. Athanassiadis, S. Rahm, A. Bergman, E.K. Wehler, Identification of hydroxylated PCB metabolites and other phenolic halogenated pollutants in human blood plasma, Arch. Environ. Contam. Toxicol. 42 (2002) 105–117.
[17] N. Quinete, A. Esser, T. Kraus, T. Schettgen, Determination of hydroxylated polychlorinated biphenyls (OH-PCBs) in human urine in a highly occupationally exposed German cohort: new prospects for urinary biomarkers of PCB exposure, Environ. Int. 97 (2016) 171–179.
[18] N. Quinete, T. Schettgen, J. Bertram, T. Kraus, Analytical approaches for the determination of PCB metabolites in blood: a review, Anal. Bioanal. Chem. 406 (2014) 6151–6164.
[19] F. Meier, S. Beck, N. Grassl, M. Lubeck, M.A. Park, O. Raether, M. Mann, Parallel accumulation-serial fragmentation (PASEF): multiplying sequencing speed and sensitivity by synchronized scans in a trapped ion mobility device, J. Proteome Res. 14 (2015) 5378–5387.
[20] F. Lanucara, S.W. Holman, C.J. Gray, C.E. Eyers, The power of ion mobility-mass spectrometry for structural characterization and the study of conformational dynamics, Nat. Chem. 6 (2014) 281–294.
[21] P. Benigni, C.J. Thompson, M.E. Ridgeway, M.A. Park, F.A. Fernandez-Lima, Targeted high-resolution ion mobility separation coupled to ultrahigh-resolution mass spectrometry of endocrine disruptors in complex mixtures, Anal. Chem. 87 (2015) 4321–4325.
[22] S.J. Valentine, M.D. Plasencia, X. Liu, M. Krishnan, S. Naylor, H.R. Udseth, R.D. Smith, D.E. Clemmer, Toward plasma proteome profiling with ion mobility–mass spectrometry, J. Proteome Res. 5 (2006) 2977–2984.
[23] S.J. Valentine, A.E. Counterman, C.S. Hoaglund, J.P. Reilly, D.E. Clemmer, Gas-phase separations of protease digests, J. Am. Soc. Mass Spectrom. 9 (1998) 1213–1216.
[24] K. Venne, E. Bonneil, K. Eng, P. Thibault, Improvement in peptide detection for proteomics analyses using nano LC–MS and high-field asymmetry waveform ion mobility mass spectrometry, Anal. Chem. 77 (2005) 2176–2186.
[25] E.W. McDaniel, E.A. Mason, Mobility and Diffusion of Ions in Gases, John Wiley and Sons, Inc., New York, New York, 1973.
[26] K.J. Gillig, D.H. Russell, A periodic field focusing ion mobility spectrometer, in: Patent Cooperation Treaty Int. Appl. WO0165589, The Texas A&M University System, 2001, pp. 36.
[27] K.J. Gillig, B.T. Ruotolo, E.G. Stone, D.H. Russell, An electrostatic focusing ion guide for ion mobility-mass spectrometry, Int. J. Mass Spectrom. 239 (2004) 43–49.
[28] J.A. Silveira, C.M. Gamage, R.C. Blase, D.H. Russell, Gas-phase ion dynamics in a periodic-focusing DC ion guide, Int. J. Mass spectrom. 296 (2010) 36–42.
[29] Y. Guo, J. Wang, G. Javahery, B.A. Thomson, K.W.M. Siu, Ion mobility spectrometer with radial collisional focusing, Anal. Chem. 77 (2004) 266–275.
[30] S.L. Koeniger, S.I. Merenbloom, S.J. Valentine, M.F. Jarrold, H.R. Udseth, R.D. Smith, D.E. Clemmer, An IMS–IMS analogue of MS–MS, Anal. Chem. 78 (2006) 4161–4174.
[31] R.T. Kurulugama, F.M. Nachtigall, S. Lee, S.J. Valentine, D.E. Clemmer, Overtone mobility spectrometry: part 1. Experimental observations, J. Am. Soc. Mass Spectrom. 20 (2009) 729–737.
[32] R.S. Glaskin, S.J. Valentine, D.E. Clemmer, A scanning frequency mode for ion cyclotron mobility spectrometry, Anal. Chem. 82 (2010) 8266–8271.
[33] S.D. Pringle, K. Giles, J.L. Wildgoose, J.P. Williams, S.E. Slade, K. Thalassinos, R.H. Bateman, M.T. Bowers, J.H. Scrivens, An investigation of the mobility separation of some peptide and protein ions using a new hybrid quadrupole/travelling wave IMS/oa-ToF instrument, Int. J. Mass Spectrom. 261 (2007) 1–12.
[34] M.F. Bush, Z. Hall, K. Giles, J. Hoyes, C.V. Robinson, B.T. Ruotolo, Collision cross sections of proteins and their complexes: a calibration framework and database for gas-phase structural biology, Anal. Chem. 82 (2010) 9557–9565.
[35] I.K. Webb, S.V.B. Garimella, A.V. Tolmachev, T.-C. Chen, X. Zhang, R.V. Norheim, S.A. Prost, B. LaMarche, G.A. Anderson, Y.M. Ibrahim, R.D. Smith, Experimental evaluation and optimization of structures for lossless ion manipulations for ion mobility spectrometry with time-of-flight mass spectrometry, Anal. Chem. 86 (2014) 9169–9176.
[36] P. Dugourd, R.R. Hudgins, D.E. Clemmer, M.F. Jarrold, High-resolution ion mobility measurements, Rev. Sci. Instrum. 68 (1997) 1122–1129.
[37] S.I. Merenbloom, R.S. Glaskin, Z.B. Henson, D.E. Clemmer, High-resolution ion cyclotron mobility spectrometry, Anal. Chem. 81 (2009) 1482–1487.
[38] P.R. Kemper, N.F. Dupuis, M.T. Bowers, A new higher resolution, ion mobility mass spectrometer, Int. J. Mass spectrom. 287 (2009) 46–57.
[39] R.C. Blase, J.A. Silveira, K.J. Gillig, C.M. Gamage, D.H. Russell, Increased ion transmission in IMS: a high resolution periodic-focusing DC ion guide ion mobility spectrometer, Int. J. Mass spectrom. 301 (2011) 166–173.
[40] J. May, D. Russell, A mass-selective variable-temperature drift tube ion mobility-mass spectrometer for temperature dependent ion mobility studies, J. Am. Soc. Mass Spectrom. 22 (2011) 1134–1145.
[41] P.R. Kemper, M.T. Bowers, A hybrid double-focusing mass spectrometer–high-pressure drift reaction cell to study thermal energy reactions of mass-selected ions, J. Am. Soc. Mass Spectrom. 1 (1990) 197–207.
[42] C. Wu, W.F. Siems, G.R. Asbury, H.H. Hill, Electrospray ionization high-resolution ion mobility spectrometry–mass spectrometry, Anal. Chem. 70 (1998) 4929–4938.
[43] Y. Liu, D.E. Clemmer, Characterizing oligosaccharides using injected-ion mobility/mass spectrometry, Anal. Chem. 69 (1997) 2504–2509.
[44] M.F. Jarrold, V.A. Constant, Silicon cluster ions: evidence for a structural transition, Phys. Rev. Lett. 67 (1991) 2994.
[45] F.A. Fernandez-Lima, D.A. Kaplan, J. Suetering, M.A. Park, Gas-phase separation using a trapped ion mobility spectrometer, Int. J. Ion Mobility Spectrom. 14 (2011) 93–98.
[46] F.A. Fernandez-Lima, D.A. Kaplan, M.A. Park, Note Integration of trapped ion mobility spectrometry with mass spectrometry, Rev. Sci. Instr. 82 (2011) 126106.

Please cite this article in press as: K.J. Adams, et al., Discovery and targeted monitoring of polychlorinated biphenyl metabolites in blood plasma using LC-TIMS-TOF MS, Int. J. Mass Spectrom. (2017), https://doi.org/10.1016/j.ijms.2017.11.009

[47] A. Castellanos, P. Benigni, D.R. Hernandez, J.D. DeBord, M.E. Ridgeway, M.A. Park, F.A. Fernandez-Lima, Fast screening of polycyclic aromatic hydrocarbons using trapped ion mobility spectrometry–mass spectrometry, Anal. Meth. 6 (2014) 9328–9332.
[48] P. Benigni, C.J. Thompson, M.E. Ridgeway, M.A. Park, F. Fernandez-Lima, Targeted high-resolution ion mobility separation coupled to ultrahigh-resolution mass spectrometry of endocrine disruptors in complex mixtures, Anal. Chem. 87 (2015) 4321–4325.
[49] E.R. Schenk, V. Mendez, J.T. Landrum, M.E. Ridgeway, M.A. Park, F. Fernandez-Lima, Direct observation of differences of carotenoid polyene chain cis/trans isomers resulting from structural topology, Anal. Chem. 86 (2014) 2019–2024.
[50] E.R. Schenk, M.E. Ridgeway, M.A. Park, F. Leng, F. Fernandez-Lima, Isomerization kinetics of AT hook decapeptide solution structures, Anal. Chem. 86 (2014) 1210–1214.
[51] J.C. Molano-Arevalo, D.R. Hernandez, W.G. Gonzalez, J. Miksovska, M.E. Ridgeway, M.A. Park, F. Fernandez-Lima, Flavin Adenine Dinucleotide structural motifs: from solution to gas-phase, Anal. Chem. 86 (2014) 10223–10230.
[52] A. McKenzie, J.D. DeBord, M.E. Ridgeway, M.A. Park, G.A. Eiceman, F. Fernandez-Lima, Lifetimes and Stabilities of familiar explosives molecular adduct complexes during ion mobility measurements, Analyst 140 (2015) 5692–5699.
[53] D.R. Hernandez, J.D. DeBord, M.E. Ridgeway, D.A. Kaplan, M.A. Park, F.A. Fernandez-Lima, Ion dynamics in a trapped ion mobility spectrometer, Analyst 139 (2014) 1913–1921.
[54] E.R. Schenk, F. Nau, F. Fernandez-Lima, Theoretical predictor for candidate structure assignment from IMS data of biomolecule-related conformational space, Int. J. Ion Mobility Spectrom. 18 (2015) 23–29.
[55] E.R. Schenk, R. Almeida, J. Miksovska, M.E. Ridgeway, M.A. Park, F. Fernandez-Lima, Kinetic intermediates of holo- and apo-myoglobin studied using HDX-TIMS-MS and molecular dynamic simulations, J. Am. Soc. Mass Spectrom. 26 (2015) 555–563.
[56] K.J. Adams, D. Montero, D. Aga, F. Fernandez-Lima, Isomer separation of polybrominated diphenyl ether metabolites using nanoESI-TIMS-MS, Int. J. Ion Mobility Spectrom. (2016) 1–8.
[57] P. Benigni, F. Fernandez-Lima, Oversampling selective accumulation trapped ion mobility spectrometry coupled to FT-ICR MS: fundamentals and applications, Anal. Chem. 88 (14) (2016) 7404–7412.
[58] P. Benigni, R. Marin, J.C. Molano-Arevalo, A. Garabedian, J.J. Wolff, M.E. Ridgeway, M.A. Park, F. Fernandez-Lima, Towards the analysis of high molecular weight proteins and protein complexes using TIMS-MS, Int. J. Ion Mobility Spectrom. (2016) 1–10.
[59] A. Garabedian, D. Butcher, J.L. Lippens, J. Miksovska, P.P. Chapagain, D. Fabris, M.E. Ridgeway, M.A. Park, F. Fernandez-Lima, Structures of the kinetically trapped i-motif DNA intermediates, Phys. Chem. Chem. Phys. 18 (2016) 26691–26702.
[60] P. Benigni, K. Sandoval, C.J. Thompson, M.E. Ridgeway, M.A. Park, P. Gardinali, F. Fernandez-Lima, Analysis of photoirradiated water accommodated fractions of crude oils using tandem TIMS and FT-ICR MS, Environ. Sci. Technol. 51 (11) (2017) 5978–5988.
[61] J.A. Silveira, M.E. Ridgeway, F.H. Laukien, M. Mann, M.A. Park, Parallel accumulation for 100% duty cycle trapped ion mobility-mass spectrometry, Int. J. Mass Spectrom. 413 (2016) 168–175.
[62] K. Michelmann, J.A. Silveira, M.E. Ridgeway, M.A. Park, Fundamentals of trapped ion mobility spectrometry, J. Am. Soc. Mass Spectrom. 26 (2015) 14–24.
[63] J.A. Silveira, K. Michelmann, M.E. Ridgeway, M.A. Park, Fundamentals of trapped ion mobility spectrometry part II: fluid dynamics, J. Am. Soc. Mass Spectrom. 27 (2016) 585–595.
[64] J.A. Silveira, W. Danielson, M.E. Ridgeway, M.A. Park, Altering the mobility-time continuum: nonlinear scan functions for targeted high resolution trapped ion mobility-mass spectrometry, Int. J. Ion Mobility Spectrom. (2016) 1–8.
[65] M.E. Ridgeway, J.A. Silveira, J.E. Meier, M.A. Park, Microheterogeneity within conformational states of ubiquitin revealed by high resolution trapped ion mobility spectrometry, Analyst 140 (2015) 6964–6972.
[66] F. Meier, S. Beck, N. Grassl, M. Lubeck, M.A. Park, O. Raether, M. Mann, Parallel accumulation–serial fragmentation (PASEF): multiplying sequencing speed and sensitivity by synchronized scans in a trapped ion mobility device, J. Proteome Res. 14 (2015) 5378–5387.
[67] J.A. Silveira, M.E. Ridgeway, M.A. Park, High resolution trapped ion mobility spectrometery of peptides, Anal. Chem. 86 (2014) 5624–5627.
[68] M.E. Ridgeway, J.J. Wolff, J.A. Silveira, C. Lin, C.E. Costello, M.A. Park, Gated trapped ion mobility spectrometry coupled to fourier transform ion cyclotron resonance mass spectrometry, Int. J. Ion Mobility Spectrom. (2016) 1–9.
[69] Y. Pu, M.E. Ridgeway, R.S. Glaskin, M.A. Park, C.E. Costello, C. Lin, Separation and identification of isomeric glycans by selected accumulation-trapped ion mobility spectrometry-electron activated dissociation tandem mass spectrometry, Anal. Chem. 88 (2016) 3440–3443.
[70] F.C. Liu, S.R. Kirk, C. Bleiholder, On the structural denaturation of biological analytes in trapped ion mobility spectrometry–mass spectrometry, Analyst 141 (2016) 3722–3730.
[71] J. Au, M.-H. Su, M. Wientjes, Extraction of intracellular nucleosides and nucleotides with acetonitrile, Clin. Chem. 35 (1989) 48–51.
[72] H. Bi, K.W. Krausz, S.K. Manna, F. Li, C.H. Johnson, F.J. Gonzalez, Optimization of harvesting, extraction, and analytical protocols for UPLC-ESI–MS-based metabolomic analysis of adherent mammalian cancer cells, Anal. Bioanal. Chem. 405 (2013) 5279–5289.
[73] M.J. Frisch, G.W. Trucks, H.B. Schlegel, G.E. Scuseria, M.A. Robb, J.R. Cheeseman, J.A. Montgomery Jr., T. Vreven, K.N. Kudin, J.C. Burant, J.M. Millam, S.S. Iyengar, J. Tomasi, V. Barone, B. Mennucci, M. Cossi, G. Scalmani, N. Rega, G.A. Petersson, H. Nakatsuji, M. Hada, M. Ehara, K. Toyota, R. Fukuda, J. Hasegawa, M. Ishida, T. Nakajima, Y. Honda, O. Kitao, H. Nakai, M. Klene, X. Li, J.E. Knox, H.P. Hratchian, J.B. Cross, V. Bakken, C. Adamo, J. Jaramillo, R. Gomperts, R.E. Stratmann, O. Yazyev, A.J. Austin, R. Cammi, C. Pomelli, J.W. Ochterski, P.Y. Ayala, K. Morokuma, G.A. Voth, P. Salvador, J.J. Dannenberg, V.G. Zakrzewski, S. Dapprich, A.D. Daniels, M.C. Strain, O. Farkas, D.K. Malick, A.D. Rabuck, K. Raghavachari, J.B. Foresman, J.V. Ortiz, Q. Cui, A.G. Baboul, S. Clifford, J. Cioslowski, B.B. Stefanov, G. Liu, A. Liashenko, P. Piskorz, I. Komaromi, R.L. Martin, D.J. Fox, T. Keith, M.A. Al-Laham, C.Y. Peng, A. Nanayakkara, M. Challacombe, P.M.W. Gill, B. Johnson, W. Chen, M.W. Wong, C. Gonzalez, J.A. Pople, Gaussian 03, Revision C.02, Gaussian, Inc, Wallingford CT, 2004.
[74] I. Campuzano, M.F. Bush, C.V. Robinson, C. Beaumont, K. Richardson, H. Kim, H.I. Kim, Structural characterization of drug-like compounds by ion mobility mass spectrometry: comparison of theoretical and experimentally derived nitrogen collision cross sections, Anal. Chem. 84 (2011) 1026–1033.
[75] H.I. Kim, H. Kim, E.S. Pang, E.K. Ryu, L.W. Beegle, J.A. Loo, W.A. Goddard, I. Kanik, Structural characterization of unsaturated phosphatidylcholines using traveling wave ion mobility spectrometry, Anal. Chem. 81 (2009) 8289–8297.
[76] U.C. Singh, P.A. Kollman, An approach to computing electrostatic charges for molecules, J. Comput. Chem. 5 (1984) 129–145.
[77] B.H. Besler, K.M. Merz, P.A. Kollman, Atomic charges derived from semiempirical methods, J. Comput. Chem. 11 (1990) 431–439.
[78] R. Letcher, H. Li, S. Chu, Determination of hydroxylated polychlorinated biphenyls (HO-PCBs) in blood plasma by high-performance liquid chromatography-electrospray ionization-tandem quadrupole mass spectrometry, J. Anal. Toxicol. 29 (2005) 209–216.
[79] L. Hovander, T. Malmberg, M. Athanasiadou, I. Athanassiadis, S. Rahm, E.K. Wehler, Identification of hydroxylated PCB metabolites and other phenolic halogenated pollutants in human blood plasma, Arch. Environ. Contam. Toxicol. 42 (2002) 105–117.

Please cite this article in press as: K.J. Adams, et al., Discovery and targeted monitoring of polychlorinated biphenyl metabolites in blood plasma using LC-TIMS-TOF MS, Int. J. Mass Spectrom. (2017), https://doi.org/10.1016/j.ijms.2017.11.009